White Noise Analysis of a Chromatic Type Horizontal Cell in the *Xenopus* Retina

SUSAN L. STONE

From the Department of Ophthalmology, New York University Medical Center, New York 10016

ABSTRACT The dynamics of color-coded signal transmission in the light-adapted *Xenopus* retina were studied by a combination of white noise (Wiener) analysis and simultaneous recordings from two types of horizontal cells: chromatic-type horizontal cells (C-HCs) are hyperpolarized by blue light and depolarized by red light, whereas luminosity-type horizontal cells (L-HCs) are hyperpolarized by all wavelengths. The retina was stimulated by two superimposed fields of red and blue light modulated by two independent white noise signals, and the resulting intracellular responses were decomposed into red and blue components (first-order kernels).

The first-order kernels predict the intracellular responses with a small degree of error (3.5–9.5% in terms of mean square error) under conditions where modulated responses exceeded 30 mV in amplitude peak-to-peak, thus demonstrating that both red and blue modulation responses are linear. Moreover, there is little or no interaction between the red- and blue-evoked responses; i.e., nearly identical first-order kernels were obtained for one color whether the other color was modulated or not. In C-HCs (but not L-HCs), there were consistent differences in the dynamics of the red and blue responses. In the C-HC, the cutoff frequency of the red response was higher than for the blue ($\sim$ 12 vs 5 Hz), and the red kernel was more bandpass than the blue. In the L-HC, kernel waveform and cutoff frequencies were similar for both colors ($\sim$ 12 Hz or greater), and the time-to-peak of the L-HC kernel was always shorter than either the red or blue C-HC kernel.

These results have implications for the mechanisms underlying color coding in the distal retina, and they further suggest that nonlinear phenomena, such as voltage-dependent conductances in HCs, do not contribute to the generation of modulation responses under the experimental conditions used here.

INTRODUCTION

Two functional classes of horizontal cells are found in the vertebrate retina: luminosity-type horizontal cells (L-HCs) are hyperpolarized by all wavelengths of visible light, whereas chromatic-type horizontal cells (C-HCs) are hyperpolarized by some wavelengths and depolarized by others. The goal of this study is to describe the

Address correspondence to Dr. Susan Stone, Dept. Ophthalmology, PHL 818, NYU Medical Center, 550 First Ave., New York, NY 10016.

J. GEN. PHYSIOL. © The Rockefeller University Press · 0022-1295/94/06/0991/27 $2.00
Volume 103 June 1994 991–1017

response dynamics of a chromatic-type horizontal cell in the intact retina of the clawed frog *Xenopus laevis*. This cell is hyperpolarized by blue light and depolarized by red light (Stone, Witkovsky, and Schütte, 1990), thus it is very similar to biphasic color–opponent horizontal cells in many vertebrate species (Svaetichin and MacNichol, 1958; Naka and Rushton, 1966*a*; Miller, Hashimoto, Saito, and Tomita, 1973; Fain, 1975; Burkhardt and Hassin, 1978; Ogden, Mascetti, and Pierantoni, 1985; Gottesman and Burkhardt, 1987; Djamgoz and Downing, 1988; Kamermans, van Dijk, and Spekreijse, 1991). Previous studies using a white noise–modulated light stimulus (Sakuranaga and Naka, 1985; Chappell, Naka, and Sakuranaga, 1985) and sinusoidal stimuli (Tranchina, Gordon, Shapley, and Toyoda, 1981; Tranchina, Gordon, and Shapley, 1983) revealed that transmission to L-HCs is linear over a wide range of mean luminance and depth of modulation, and Spekreijse and Norton (1970) used sinusoidal stimuli and linear system analysis to investigate C-HC response dynamics in the carp. Because there have been few studies addressing the issue of C-HC response dynamics, there is no basis for assuming that the dynamic behavior of the two HC types will be similar, especially when one considers that the mechanism(s) underlying color opponency in C-HCs is uncertain.

White noise (Wiener kernel) analysis is an efficient tool for defining the dynamic features and input–output relation of a system. The Gaussian white noise signal is an information-rich stimulus; it contains all of the frequencies to which a cell is capable of responding. A white noise–modulated light stimulus is particularly well suited for vision research because a modulation around a mean luminance closely resembles a general visual stimulus in the natural environment. The concept of functional identification of a system originated with the mathematicians Volterra (1959) and Fréchet (1910) who sought to describe the output of a finite memory system by a series of Volterra functionals. Subsequently, Wiener (1958) conceived of using a general stochastic process or chaotic input (i.e., a Gaussian white noise signal) as a tool for probing a system. This method is essentially a "black box" approach; i.e., the system is defined by its transfer characteristics without specifying any information concerning the underlying biophysical mechanisms. The kernels produced by the analysis are a concise mathematical description of the filter responsible for transforming the input into the output. The ability to define a neuron or a network by what it is doing, without knowing precisely how it is doing it, is of value if one is to understand the role of specific synaptic pathways, individual synapses, and ion channels (usually studied in isolated cell cultures or tissue slices). A major advantage of applying this technique in the eyecup preparation is that the dynamic behavior of retinal neurons can be studied in the light with the entire retinal network intact. Because the retina processes color/contrast information in the light, not in the dark, the experimental conditions used here approximate the in vivo situation in which the animal is actually seeing.

White noise analysis has been used most extensively in characterizing the retinal neuron network (Marmarelis and Naka, 1972; reviewed in Sakai and Naka, 1987, 1988; Naka and Sakai, 1991; Sakai, 1992), auditory system (Eggermont, 1993), and many areas of neurophysiology (Kondoh, Arima, Okuma, and Hasegawa, 1993; Weckström, Kouvalainen, and Juusola, 1992; Jacobson, Gaska, Chen, and Pollen, 1993). Unlike conventional (i.e., linear) system analysis, it is capable of identifying

both the linear and nonlinear components of a response. Other laboratories have adopted closely related cross-correlation techniques for characterizing the visual system (reviewed by Victor, 1992), such as an M-sequence modulation, a random binary input (Sutter, 1987; Collins and Sawhney, 1993), sum of sinusoids (Victor and Knight, 1979; Victor and Shapley, 1979), or random checkerboard patterns (Jones and Palmer, 1987; Reid and Shapley, 1992; DeAngelis, Ohzawa, and Freeman, 1993).

In the present report, the dynamic features of color-coded signal transmission in the distal *Xenopus* retina were investigated by a combination of white noise analysis and simultaneous intracellular recordings from C- and L-HCs. Under conditions in which the retina was exposed simultaneously to a field of red and blue light, the following new findings were obtained: (*a*) The transmission of both red and blue signals to *Xenopus* C-HCs (and L-HCs) is linear; even under conditions in which modulation responses exceed 30 mV in amplitude, peak-to-peak. (*b*) There is little or no interaction between the red and blue signals. (*c*) In the C-HC, the frequency response of the blue signal is significantly slower than for the red signal, and the red kernel is more bandpass than the blue. (*d*) The linear behavior of the red and blue modulation responses, as well as their amplitude, does not appear to depend greatly on the level of mean membrane potential in the C-HC or L-HC. (*e*) The time-to-peak of the hyperpolarizing first-order kernel in L-HCs is shorter than the time-to-peak of either the red (depolarizing) or blue (hyperpolarizing) first-order kernel in the C-cell. These results, which could not be demonstrated in our earlier study (Stone et al., 1990) because the light stimulus was not well suited to a quantitative analysis, are discussed in terms of the currently held views on the mechanisms underlying color opponency in the distal retina.

MATERIALS AND METHODS

Experiments were performed on the light-adapted superfused eyecup preparation of the clawed frog *Xenopus laevis*. In *Xenopus*, "light-adapted" is defined as the condition in which there is no detectable green-sensitive, rod-mediated responses in second-order neurons, which receive mixed inputs from rods and cones in this species (Stone and Witkovsky, 1984; Witkovsky and Stone, 1987; Witkovsky, Stone, and Besharse, 1988). Adult *Xenopus* obtained from NASCO (Ft. Atkinson, WI) were anesthetized by a subcutaneous injection of 20–30 mg of ethyl *m*-aminobenzoate, the eye was enucleated in room light, and the animal was euthanized by pithing and decapitation. The retina-eyecup preparation was exposed to continuous background illumination (red plus blue) to maintain light adaptation at a steady state level (described in more detail below). Intracellular recordings from C-HCs and L-HCs were obtained conventionally and stored on an eight-channel PCM VCR recorder (model 5000; A. R. Vetter Co., Inc., Rebersburg, PA), as described previously (Stone et al., 1990). 15 C-HCs (and >50 L-HCs) from 15 different retinas were studied. Cells were identified by the waveform, and polarity of the response evoked by red and blue light steps and five C-HCs were further identified by intracellular dye injection with horseradish peroxidase. In four experiments, simultaneous intracellular recordings from a C-HC and nearby L-HC were obtained.

Light Stimulation

Except for the data shown in Fig. 4, light stimulation was provided by red (660 nm; Stanley Super-Brite, Hamamatsu Corp., Bridgewater, NJ) and blue (470 nm; Cree, 101CR-ND

Digi-Key Corp., Thief River Falls, MN) light emitting diodes (LED) driven by independent LED drivers (a voltage to current converter constructed in the New York University electronics shop). The LED driver was used to adjust the mean level of illumination and had an input for modulation around the mean level. Each LED illuminated the entire retina. The quantal flux of each light source was measured periodically by a quantum sensor (no. LI-190SA; Li-Cor., Inc., Lincoln, NE) placed in the plane of the retina. The maximal quantal flux of the red LED was 25×10^{14} photons·cm^{-2}·s^{-1}, and that of the blue LED was 8×10^{12} photons·cm^{-2}·s^{-1}; however, the range of the mean light intensities used in most experiments was between 10^{11} and 3×10^{12} photons·cm^{-2}·s^{-1}. These values, in units of photons·cm^{-2}·s^{-1}, are given in the figure legends.

To generate a modulated input, each LED was connected to a swept sinewave function generator (no. FG 507; Tektronix, Inc., Beaverton, OR) or independent channels of a white noise function generator (no. 1360; NF Electronic Instruments, NF Circuit Design Block Co. Ltd., Tokyo, Japan) that also controlled the bandwidth and power of the white noise stimulus. Alternating red and blue light steps were used when searching for cells. The light output of each LED was recorded by independent photodiodes (no. S1406; Hamamatsu Photonic Sys. Corp., Bridgewater, NJ) placed close to each light source, which were well shielded from each other to prevent cross-talk between the separate inputs. The photodiode signal corresponds to the stimulus record in the figures and served as the input signal for the computer analysis.

Although an ideal Gaussian white noise signal contains all frequencies with equal power, the white noise input used in these studies was band limited (DC-30 Hz). The amplitude distribution of the white noise input (and output) is called the probability density function (PDF). The PDF $p(x)$, when multiplied by an infinitesimal interval length $d(x)$ gives the probability that the sampled variable falls between x and $x + dx$. As shown in Fig. 1, the PDF of the white noise inputs used in this study closely approximates a Gaussian function; the solid line in Fig. 1 shows the best Gaussian fit superimposed on the PDF. The PDF was used to estimate the depth of modulation of the white noise input, taking three standard deviations to represent dimmer and brighter limits of the light stimulus. Depth of modulation is defined as

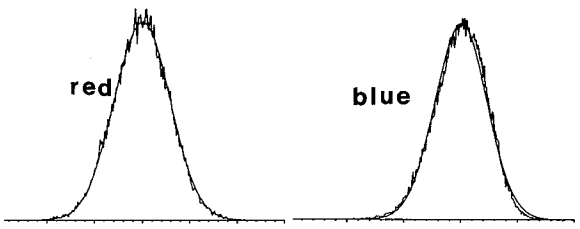

FIGURE 1. Power density function (PDF) of red (*left*) and blue (*right*) white noise inputs (DC to 30 Hz). The amplitude of the modulation response increases from left (0% modulation) to right (100% modulation) on the abscissa. Solid line is best Gaussian fit to the data. See text for further explanation.

$$(L_{max} - L_{min})/(L_{max} + L_{min}),$$

where L is light intensity as estimated from the PDF abscissa. In different experiments, the modulation depth of the inputs varied from 25 to 76%; these values are given in the figure legends. The values given for the depth of modulation of the white noise signals are only an approximation because of the statistical nature of the input.

The protocol used for setting the mean level of illumination and for recording routine light responses is illustrated in Figs. 2 and 3. In Fig. 2*A*, the top trace shows a continuous intracellular C-HC recording as a red or blue mean luminance was turned ON and OFF. In this cell, the "dark" membrane potential was ~ -25 mV. When the blue mean alone was "ON," the

C-HC hyperpolarized to ~−68 mV; when the red mean alone was turned ON, the cell depolarized to ~0 mV, and when both the red and blue means were ON simultaneously, the cell polarized to a stable intermediate level, in this case, ~−40 mV. For the white noise experiments presented in this report, the retina was exposed continuously to a steady red and blue luminance which, depending on intensity, polarized the C-HC to between −30 and −50 mV in the steady state. Fig. 2 *B* shows light responses from this cell evoked by 200-ms red and blue light steps flashed from the "dark" level, i.e., no mean luminance.

Fig. 3 illustrates part of the stimulation regimen used in the white noise modulation experiments (different retina than in Fig. 2). The red and blue inputs were modulated in various combinations. The top traces in Fig. 3 *A* are samples from a continuous 8-min

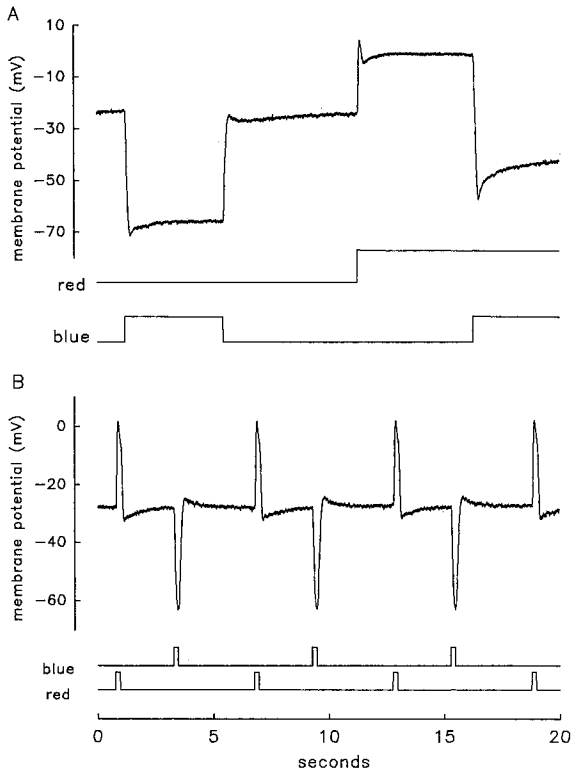

FIGURE 2. Intracellular recording from a C-HC in response to sustained illumination and 200-ms steps evoked by red (660 nm) and blue (470 nm) light. The C-HC is depolarized by red light and hyperpolarized by blue light. The mV scale in (*A*) and (*B*) refers to the intracellular membrane potential. Stimulus traces labeled "red" and "blue" are beneath the intracellular records. (*A*) shows a red and blue mean luminance presented separately and simultaneously. Quantal flux (photons × 10^{12}·cm^{-2}·s^{-1}): red = 3.23, blue = 5.0. (*B*) Responses evoked by light steps flashed on a dark background. Quantal flux (photons × 10^{12}·cm^{-2}·s^{-1}): red = 24.0, blue = 3.23.

intracellular recording, and the traces beneath, labeled "red" and "blue," are the light stimulus. The "fluctuating" portions of these records indicate the white noise stimulus and resulting response. In the left panel, the retina was exposed to blue white noise modulated in the presence of a steady red mean; then the red mean was turned off. In the middle panel, both blue and red means were turned off briefly, then the red mean alone was turned on. Fig. 3 *A* (*arrow*) indicates the dark potential in the absence of red or blue mean illumination. In the right panel, the cell was stimulated with red white noise–modulated light in the absence of a blue mean, and then the blue mean was turned on. Note that the total excursion in mean membrane potential under these different stimulation conditions is close to 50 mV, yet the

amplitude of the modulation responses are not greatly affected by such large changes in the mean membrane potential.

Fig. 3 *B* (*top trace*) shows red and blue step-evoked responses recorded from this cell in the presence of a steady red plus blue mean luminance. The first part of the trace shows the response during simultaneous stimulation by two independent white noise inputs (labeled "red" and "blue" in Fig. 3 *B*). Then the red and blue white noise was stopped before stimulation with red and blue light steps flashed on top of the mean. In this figure, the separate stimulus records for the red (upward deflection) and blue (downward deflection) step inputs were combined into one trace (labeled "step" in Fig. 3 *B*).

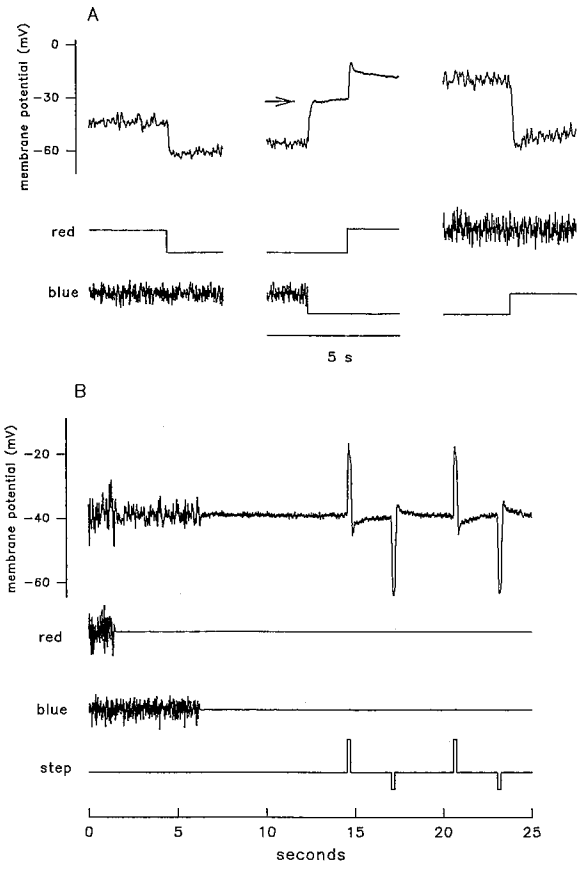

FIGURE 3. Part of the stimulation regime used in the white noise experiments. The mV scale is for the intracellular membrane potential. (*A*) The blue or red input was modulated while a mean luminance by the opponent color was turned on and off. Note that the modulation responses are not greatly altered by large changes in the mean membrane potential. Arrow indicates dark membrane potential. See text for further explanation. (*B*) Responses evoked by red and blue light steps superimposed on a dual input mean luminance (red plus blue) after stopping the modulated input. Upward deflection on stimulus trace is for the red step, and downward deflection is for the blue. Quantal flux (photons × 10^{12}·cm^{-2}·s^{-1}): (*A*) red mean = 3.23, blue mean = 1.08. Modulation depth for red and blue white noise inputs ~52%. (*B*) red step = 12, blue = 8. Mean intensity the same as in (*A*).

Data Acquisition and Analysis

Four channels of data were digitized (500 Hz) online or offline on an Axotape system (TL-40; Axon Instruments, Foster City, CA) for 60–120 s. White noise analysis was performed offline on a 386 IBM compatible personal computer (PC) using the Spatio-Temporal Analysis Routines (STAR) algorithms developed by Sakuranaga and Naka (1985). The STAR routines were translated from FORTRAN into the C language for use with MS-DOS–based PCs. Raw Axotape data was filtered (0.1–50 Hz).

First-order kernels were computed by cross-correlating the photodiode signal (input) against the intracellular response of the cell (output). Kernel amplitudes, in mV/photons × 10^{12}·cm^{-2}·s^{-1}, are given in the figure legends. The first-order prediction (linear model) was computed by convolving the light stimulus (input signal) with the first-order kernel, and power spectra and mean square error (MSE) were calculated from the filtered input, output, and predicted data, as described in the text. Second-order kernels, which represent the nonlinear component of a cell's response, were poorly defined because responses were essentially linear and are not considered here.

Overview of Wiener Kernel Analysis

The first-order Wiener kernel refers to the first-order cross-correlation between the input (white noise–modulated light stimulus) and output (intracellular response of the cell), weighted by the power of the input. It has been well established that for the linear range of a cell's response, the first-order kernel is equivalent to the cell's impulse response, i.e., the response to a brief pulse of light superimposed on a steady illuminance that corresponds to the mean of the Gaussian input. It is a function of the time lag between the input and the output.

The Gaussian white noise light stimulus $L(t)$ has two components, the mean luminance I_0 and the time-varying modulation $I(t)$. Similarly, the horizontal cell response is composed of two components, the steady polarization V_0 produced by I_0 (the synapse must be capable of transmitting a sustained DC signal) and the time-varying part $v(t)$ produced by $I(t)$.

$$V(t) = V_0(I_0) + v(t)$$

In a linear or quasilinear system, $v(t)$ can be expressed as the convolution integral:

$$v(t) = \int_0^\infty h(\tau; I_0) I(t - \tau)\, d\tau,$$

where $h(\tau; I_0)$ is the first-order kernel, and $I(t)$ is the arbitrary stimulus. The amplitude of the kernel is independent of the amplitude of the modulated input signal.

The amplitude of the first-order kernel is a measure of the cell's incremental sensitivity. The incremental sensitivity $S_i(t)$ is the relationship between a response, $\Delta V(t)$ and the input modulation $\Delta I(t)$ around a mean luminance I_0. As noted above, the first-order kernel $h(\tau; I_0)$ is obtained by cross-correlating the input against the output. If the actual quantal flux of the input signal used for the cross-correlation is known, then at a given mean luminance I_0 the incremental sensitivity is defined as:

$$S_i(t) = \Delta V(t)/\Delta I = h(\tau; I_0).$$

If two or more kernels are compared by cross-correlating the input signal before the light has been attenuated (or incremented) by one or more neutral density filters (as in Fig. 10 *B*), then the kernel amplitude scale defines the cell's contrast sensitivity. In this situation, the amplitude of the input signals used for the cross-correlation computation do not directly reflect the absolute value of the white noise modulation. This is a more practical and convenient approach when the same cell is tested at several different mean light intensities during the course of a single experiment. However, if the value of the neutral density filter is known, contrast sensitivity units can easily be converted to incremental sensitivity units by a simple multiplication factor, as described in detail by Chappell et al. (1985).

The first-order prediction (linear model) is the response of the cell predicted by the first-order kernel. The first-order prediction is obtained by convolving the white noise input signal with the first-order kernel. The MSE is a percentage measure of the deviation of the predicted response from the real intracellular response. Thus, the MSE is a measure of the

accuracy of the first-order model and is also a measure of the nonlinearity of cell's response (Sakuranaga and Naka, 1985; Sakai and Naka, 1987). In this study, the MSEs of the linear model ranged from 3.5 to 9.6%. Second-order kernels define the nonlinear component of a cell's response, however, second-order Weiner kernels are not considered in this report because as shown below, modulation responses in *Xenopus* C-type horizontal cells are essentially linear under the stimulation conditions used here. This excludes any possibility of a significant second-order component in the modulation response. A recent review of the theoretical basis for the application of white noise and related techniques in visual system identification has been published by Victor (1992).

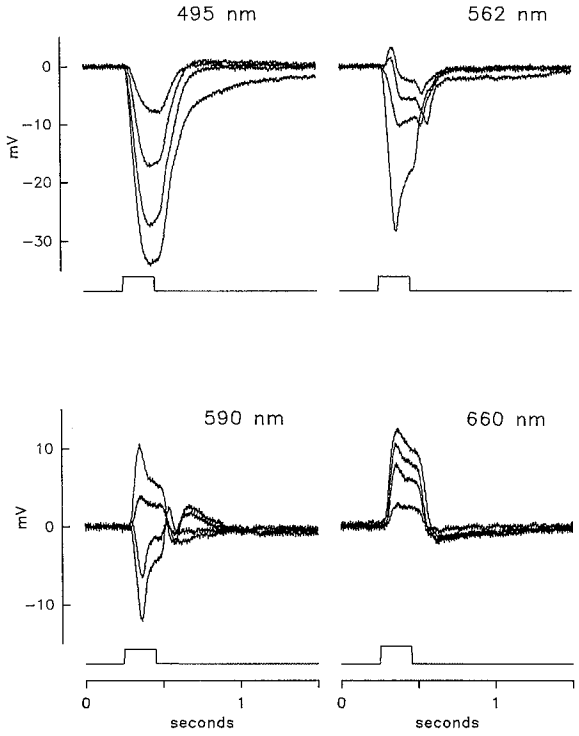

FIGURE 4. Superimposed responses of a C-HC evoked by 200-ms flashes at four different wavelengths of approximately equal quantal flux presented on a dark background. In this figure the stimulus was a quartz iodide light source filtered with narrow band interference filters (Stone et al., 1990). Flashes attenuated in steps of 0.41–0.82 log units. Maximum quantal flux ~2.3 × 10^{13} photons·cm^{-2}·s^{-1}. 0 on the mV scale corresponds to the cells dark membrane potential (−40 mV).

RESULTS

General Features of Step and Modulation Responses in C-type Horizontal Cells

The C-HC in the *Xenopus* retina is an axonless horizontal cell whose physiological response depends on stimulus wavelength (Stone et al., 1990). As shown in Figs. 2 and 3, this cell is hyperpolarized by blue light and depolarized by red light. Traditionally, color coding in this neuron has been analyzed using steps of light flashed in the dark (Naka and Rushton, 1966*b*). Fig. 4 illustrates such an experiment in an eyecup preparation that was light-adapted (i.e., no evidence of rod input) but was not exposed to any background illumination. This commonly used stimulation paradigm represents a static or non–steady state condition, a situation that is rarely encountered by an animal in its natural environment. It is difficult to quantify the

dynamic features of a response when the stimulus is a sudden increase in light intensity from the dark level.

This cell was stimulated with increasing intensity light flashes at four different wavelengths of approximately equal quantal flux. At 495 and 660 nm, the waveforms are purely hyperpolarizing and depolarizing respectively, even at saturating light intensities. When light flashes are presented on a dark background, the blue response often exceeds the red response in amplitude. However, as shown in Figs. 2 and 3 (see also Fig. 1 in Stone et al., 1990), in the presence of blue or green background illumination, both step-evoked waveforms often approach 30 mV. Often the red and blue waveforms differ in their dynamics, but these differences are variable and difficult to quantify when steps of light are used as the stimulus. At intermediate wavelengths, both spectral mechanisms contribute to the waveform. At 562 nm, the hyperpolarizing mechanism predominates, but a small depolarizing component can be seen to precede the hyperpolarization at lower light intensities. At 590 nm, the depolarizing response predominates for dim and moderate intensity stimuli, and the waveform becomes mainly hyperpolarizing at the brightest light intensities. The straightforward conclusions reached in this study contrast with the complex responses evoked by step inputs.

Fig. 5 illustrates the experimental paradigm in which the light stimulus was a modulation around a mean luminance. The eyecup was exposed simultaneously to red and blue full-field illumination, and each colored input was modulated by two independent signals. In this and all subsequent figures, the top trace in each record shows the intracellular response of the C-HC, and the small amplitude trace beneath is the photodiode signal. In Fig. 5 *A*, a swept sinewave stimulus (labeled "Red" and "Blue") was presented in the presence of steady mean (unmodulated) illumination by the other color. Fig. 5 *B* and *C*, show modulation responses from this C-HC when red (Fig. 5 *B*) and blue (Fig. 5 *C*) Gaussian white noise was the light stimulus. As for sinusoidal stimulation, the red input was modulated in the presence of an unmodulated blue mean, and the blue input was modulated in the presence of an unmodulated red mean. In this and all similar figures, the millivolt scale next to the output trace refers to the amplitude of the intracellular response, where 0 corresponds to the cell's mean membrane potential in the presence of the mean luminance. First-order Weiner kernels computed by cross-correlating each input against the output are shown in Fig. 5 *E*. The red kernel was computed by cross-correlating the red white noise stimulus (Fig. 5 *B*, *bottom trace*) against the response of the cell (Fig. 5 *B*, *top trace*), and the blue kernel was computed similarly, from the data shown in Fig. 5 *C*. Both kernels are displayed on the same amplitude (incremental sensitivity) and time scale. Note that the red kernel is depolarizing, whereas the blue kernel is hyperpolarizing.

Close inspection of the white noise modulation responses in Fig. 5, *B* and *C* (*top traces*) reveal that these records consist of two superimposed traces. The solid line is the real intracellular response, and the dotted line is the first-order (linear) model computed by convolving each (colored) input with its respective kernel from Fig. 5 *E*. This close match between the response and prediction (MSE = 5.5%) indicates that transmission of red and blue signals to the C-HC is linear. Fig. 5 *D* shows the power spectra of the white noise stimulus and response computed from the data in Fig. 5, *B*

and *C*. The two spectra marked "input" are for the red and blue white noise light stimulus; they are flat from near DC to 30 Hz. The two spectra marked "output" are for the red (*solid line*) and blue (*dashed line*) modulation response. The response spectra have been displaced along the vertical axis for clarity. In this cell, the frequency response of the blue output is significantly slower than for the red. The

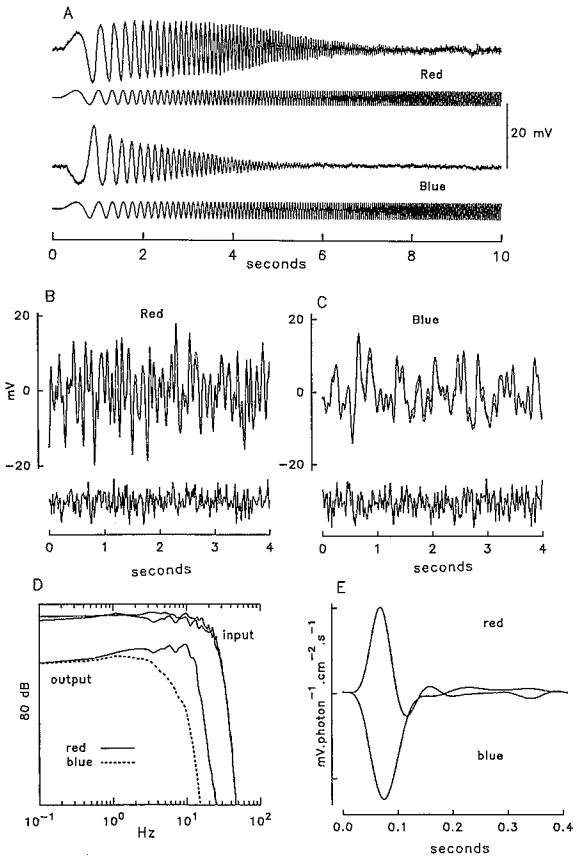

FIGURE 5. Single input white noise experiment. The retina was exposed to continuous mean illumination (red plus blue), and each input was modulated separately in the presence of an unmodulated mean luminance of the opponent color. (*A*) Response to red and blue swept sinewave input. (*B*) Red white noise input and resulting modulation response in the presence of a blue mean luminance. (*C*) Blue white noise input and resulting modulation response in the presence of a red mean luminance. Modulation depth ~76% in (*A*) and (*B*). (*D*) Power spectra computed from data in (*B*) and (*C*) plotted on the same decibel scale. The response traces have been displaced along the vertical axis for clarity. (*E*) First-order Weiner kernels computed from data in (*B*) and (*C*) by cross-correlating each input against the resulting response. The red (depolarizing) and blue (hyperpolarizing) kernels are plotted on the same amplitude (incremental sensitivity) scale. The first-order (linear) model was computed by convolving each input (*B* and *C*, *bottom traces*) with the first-order kernels in (*E*) as described in the text. The predicted responses (*dotted traces*) are superimposed on the real intracellular response (*solid traces*) in the response records of (*B*) and (*C*). Mean light intensity for all records in photons × 10^{12}·cm^{-2}·s^{-1}: red = 3.23, blue = 3.23. Kernel units: (mV/photon × 10^{12}·cm^{-2}·s^{-1}) = 275.

cutoff frequency for the red response is ~12–14 Hz, whereas the blue response falls off at ~4–5 Hz. These differences in the frequency response are also revealed by comparing the width and time to peak of the red and blue kernels in Fig. 5 *E*.

An example of a dual input experiment (different cell than in Fig. 5) is illustrated in Fig. 6. Two independent white noise inputs were presented simultaneously and as

separately. Fig. 6, *A* (red) and *B* (blue), show the white noise stimulus and resulting response when each color was presented separately in the presence of an unmodulated mean luminance by the opponent color. The response records in Fig. 6, *A* and *B* also consist of two superimposed traces, the real intracellular response (*solid line*) and the first-order prediction (*dotted line*). Fig. 6 *C* shows the intracellular response when the red and blue white noise inputs (*bottom two traces*) were modulated simultaneously. In Fig. 6 *D*, two sets of first-order kernels are displayed on the same incremental sensitivity scale. The solid-line kernels were computed from the separate input data (Fig. 6, *A* and *B*) and were used for the first-order convolution. The

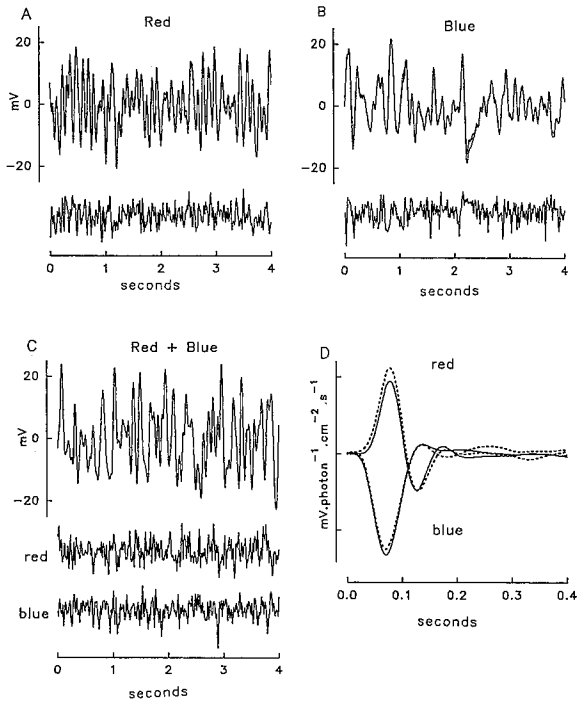

FIGURE 6. Dual input white noise experiment (different retina than in Fig. 5). Two independent white noise inputs were presented simultaneously and separately. (*A*) Red white noise input and resulting response (*solid trace*) and first-order prediction (dotted trace) in the presence of an unmodulated blue mean luminance. MSE = 6.1% (*B*) Blue white noise input and resulting response (*solid trace*) and first-order prediction (*dotted trace*) in the presence of an unmodulated red mean luminance. MSE = 4.6%. (*C*) Intracellular response evoked by red and blue white-noise inputs presented simultaneously. (*D*) First-order Weiner kernels computed from the data in *A–C* plotted on the same incremental sensitivity scale. The solid-line kernels are for the separate inputs (*A* and *B*) and the dashed-line kernels are for the mixed inputs (*C*). Modulation depth in A–C is ~59%. Mean light intensity in photons × 10^{12}·cm^{-2}·s^{-1}: red = 3.23, blue = 3.23. Kernel units: (mV/photon × 10^{12}·cm^{-2}·s^{-1}) = 280.

dashed-line kernels were computed from the dual input data in Fig. 6 *C*. That is, the red stimulus in Fig. 6 *C* was cross-correlated against the response of the cell to produce the red kernel, and the blue stimulus was cross-correlated against the same intracellular response to produce the blue kernel. The finding that the two sets of kernels for separate or mixed inputs are nearly identical indicates that there is little or no interaction between the red and blue modulation responses.

The responses of this cell to red and blue sinewave stimuli are shown in Fig. 7 *A*, and the power spectra computed from the white noise data (Fig. 6, *A* and *B*) are shown in Fig. 7 *B*. The power spectra of the red and blue stimuli are indicated by the

two curves labeled "input," and the spectra of the real and predicted responses are indicated by the four curves labeled "output." For the case of the output spectra, the solid-line (red) and dashed-line (blue) curves depict the real intracellular responses, whereas the dotted curves show the power spectra for the predicted responses computed from the linear model (Fig. 6, *A* and *B, dotted traces*). It is evident that the power spectra for real and predicted responses match very closely, as do the real and predicted intracellular responses from which these power spectra were computed.

In a linear system, the first-order kernel defines the filter responsible for transforming the input into the output. Thus, it should be possible to predict a cell's

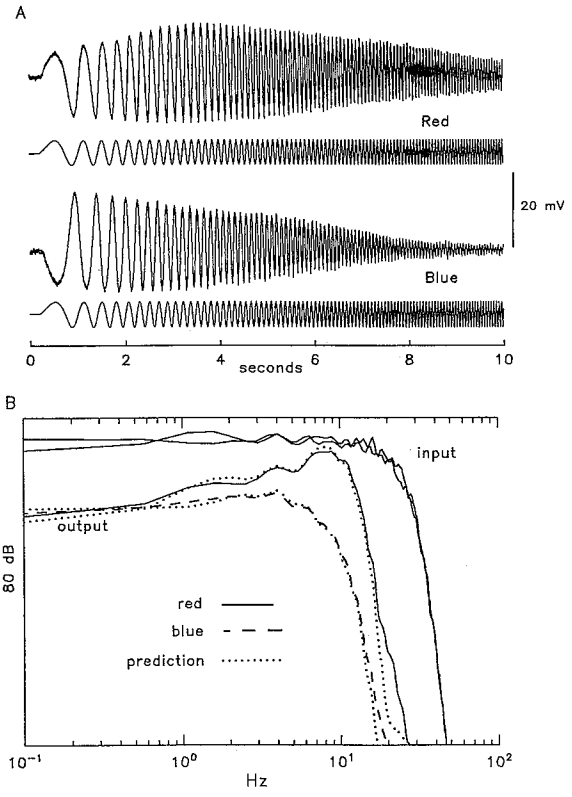

FIGURE 7. (A) Response evoked by red and blue swept sinewave stimulus in presence of a mean luminance of the opponent color. Same cell as in Fig. 6. Mean light intensity in photons × 10^{12}·cm^{-2}·s^{-1}: red = 32.3, blue = 3.23. (*B*) Power spectra computed from the white noise data in Fig. 6, *A* and *B*. The two spectra marked "input" are for the red and blue stimulus; the four spectra marked "output" are for the red modulation response (*solid line*), the blue modulation response (*dashed line*), and the first-order predictions (*dotted lines*). The spectra are plotted on the same decibel scale but the output curves have been displaced along the vertical axis for clarity. Fig. 2 *B* shows the response of this cell evoked by red and blue light steps.

response to any input that falls within the range of the modulation responses used for computing the kernel. This point is illustrated in Fig. 8, which shows responses evoked by a red and blue sine wave stimulus (Fig. 8 *A*) and a 200-ms incremental step from the mean luminance (Fig. 8 *B*). Fig. 8 *C* shows first-order kernels computed from white noise light stimulation at the same mean intensity used for the sine wave and step inputs. (The white noise data that produced the kernels is not illustrated.) The linear model was computed by convolving the sinewave and step inputs (Fig. 8, *A* and *B*, lower traces) with the red (left) and blue (right) first-order kernels in Fig. 8 *C*. The predicted response is displayed as the superimposed dashed trace in the

response records of Fig. 8, *A* and *B*. Even for the case of step responses generated by a sudden increase from the mean luminance, the linear prediction and real intracellular responses still match fairly closely. All of this strongly supports the conclusion that transmission of red and blue signals to the C-type horizontal cell in *Xenopus* in linear for responses up to ±20 mV from the mean membrane potential.

To summarize briefly from the results presented so far in Figs. 5–8, the following interpretations can be made: (*a*) transmission of red and blue signals to the C-HC is linear, even for modulation responses exceeding 30 mV peak-to-peak. Thus, the

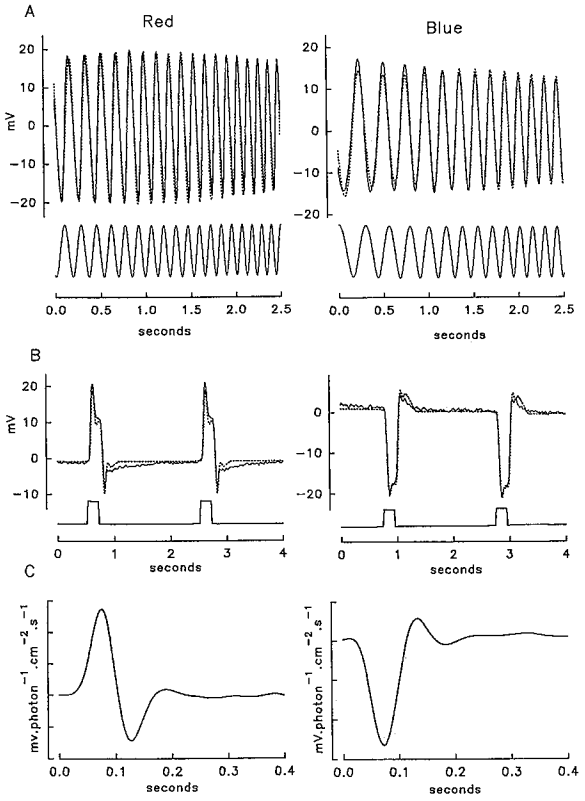

FIGURE 8. Application of first-order (linear) model to sinewave and step-evoked responses. (*A* and *B*) Responses evoked by a red (*left*) and blue (*right*) sinewave stimulus and incremental steps from one mean in the presence of a mean luminance by the opponent color. (*C*) Red (*left*) and blue (*right*) first-order kernels computed from white noise inputs and outputs (not illustrated) at the same mean luminance used for the sinusoidal and step responses. The first-order prediction (*A* and *B*, *dotted traces*) was computed by convolving the sinewave and step stimuli (*A* and *B*, *lower traces*), with the first-order kernels in *C*. Mean light intensity in photons × 10^{12}·cm^{-2}·s^{-1}: red = 32.3, blue = 3.23. Sinewave modulation depth ~66%, step increments ~70% from mean. Kernel units (mV/photon × 10^{12}·cm^{-2}·s^{-1}): red = 13, blue = 55.

first-order kernel is an accurate description of the filter responsible for transforming the input into the output.

(*b*) At a given mean luminance, there is little interaction between the red and blue modulation responses. In other words, under these steady-state conditions, the response dynamics of the red C-HC signal are not influenced by the blue, and vice versa. This is verified by the nearly identical kernels produced by single input or dual input stimulation in Fig. 6 *D*.

(*c*) In general, there were significant differences in the frequency response of the red and blue C-HC signals. The power spectra in Figs. 5 *D* and 7 *B* clearly reveal that the red output signal follows faster input frequencies than the blue output. This is also obvious during sinusoidal stimulation in Figs. 5 *A* and 7 *A*. Also, closer examination of the red and blue kernels reveals that the red kernel is more band pass than the blue kernel. Thus, despite the fact that red and blue step-evoked waveforms of C-HCs are often similar in waveform (except for their polarity), the white noise analysis reveals there are small but consistent differences in the dynamics of their modulation responses.

(*d*) The analysis is capable of isolating the separate response components resulting from a complex input signal; in this study, simultaneous stimulation by two different colors. This is most clearly demonstrated by comparing the data and respective kernels in Fig. 6. In catfish bipolar cells, it was shown that white noise analysis can separate center and surround responses evoked by two simultaneously modulated spot and annular stimuli (Sakuranaga and Naka, 1985; Sakai and Naka, 1988), and more recently, it was used to isolate the separate color-coded components in the spike discharges of ganglion cells (Sakai, Naka, and Korenberg, 1992). Also, in *Xenopus* L-HCs, the analysis can isolate rod- and cone-mediated response components under mesopic conditions of adaptation (unpublished data).

Effect of Modulation Depth

If color-coded transmission to the C-HC is linear, then at a given mean luminance, changes in the modulation depth of the input signal will change the amplitude of the modulation responses, but should not alter their dynamics, including incremental sensitivity; i.e., kernels must be identical for any depth of modulation. This point is illustrated in Fig. 9, which shows a dual-input experiment during which the level of the mean luminance was held constant while the modulation depth of the red and blue input signals was varied. All of the input and output data is displayed on the same amplitude scale; the red input signal is displayed above the blue. In Fig. 9 *A*, the modulation depth of both inputs was 24%, in *B*, both inputs were modulated at 52%, and in *C*, the red input was modulated at 24%, while the blue input was modulated at 52%. The six kernels produced by cross-correlating each input against the intracellular response are shown to the right of the white noise data; the red kernels are on top and the blue kernels underneath. The three pairs of kernels resulting from the three different stimulation conditions are nearly indistinguishable in both amplitude and waveform, even for the case of simultaneous stimulation by red and blue inputs modulated at different depths (Fig. 9 *C*). This result is what one would expect from a linear system. The incremental sensitivity of the C-HC to both red and blue stimuli does not vary under steady state conditions, i.e., the mean luminance is not changing, only the modulation around the mean.

Changes in the Mean Luminance

In several species, it has been shown that the response dynamics of cones (Naka, Itoh, and Chappell, 1987), L-HCs, and bipolar cells (Naka et al., 1979; Chappell et al., 1985; Tranchina et al., 1983, 1984; Sakai and Naka, 1987) depend on the magnitude of the mean luminance. For example, in turtle L-HCs, Chappell et al. (1985) found

that increases in the mean luminance result in three major changes: (*a*) a decrease in the kernel amplitude, i.e., incremental sensitivity decreases; (*b*) the waveforms change from monophasic (integrating) to biphasic (differentiating, i.e., they become more bandpass); and (*c*) the time to peak becomes shorter and the cells respond to higher frequencies. In *Xenopus* L-HCs (under light-adapted conditions), when the intensity of the mean luminance is varied, the changes in response dynamics are very similar to those reported in turtle retina (unpublished data). It was not possible to undertake such an extensive investigation of C-HCs, thus it is uncertain whether C-HC behavior

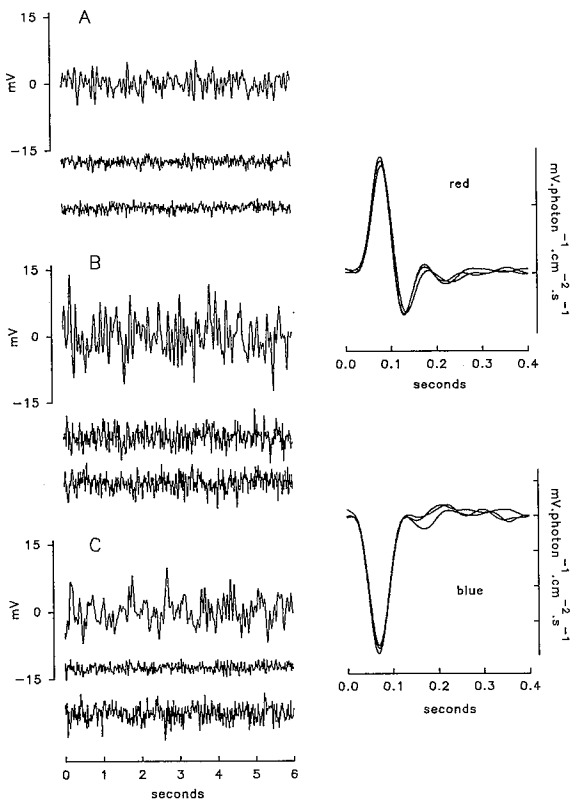

FIGURE 9. Dual input white noise experiment at different depths of modulation (24 and 52% as described in the text). (*A–C*) Simultaneous red and blue white noise inputs and resulting response from the same C cell. The mean light intensities were identical in all three records, only the depth of modulation was varied. The input and output records in *A–C* are displayed on the same amplitude and time scale. The red stimulus trace is above the blue in each record. The panels on the right show three red kernels (*top*) and three blue kernels (*bottom*) computed from the data in A–C, and are plotted on the same incremental sensitivity scale. The nearly identical amplitude and waveform of the red and blue kernels indicate that incremental sensitivity and response dynamics of this C cell is unaffected by changes in modulation depth. Mean light intensity in photons × 10^{12}·cm^{-2}·s^{-1}: red = 3.2, blue = 1.1. Kernel units (mV/photon × 10^{12}·cm^{-2}·s^{-1}): red = 80, blue = 70.

is Weber-Fechner–like, as is the case for turtle L-HCs (Chappell et al., 1985). However, the effect of varying the mean luminance was examined at two or three different intensities. Three types of stimulus conditions were used: (*a*) Changing the mean luminance of one modulated color while the mean luminance of the opponent color remained constant, (*b*) modulating one color in the absence of mean illumination by the opponent color, and (*c*) modulating one color at a constant mean luminance while the mean luminance of the opponent (unmodulated) color was varied.

Fig. 10 is an example of an experiment in which the mean intensity of the modulated input was varied by one log unit while the mean luminance of the opponent color was held constant. In Fig. 10 *A*, the bottom traces are the white noise input signal at two mean intensities (the amplitude of the right and left input signal is the same because the light detector was not measuring the effect of the neutral density filters). The top traces are the resulting intracellular response and linear

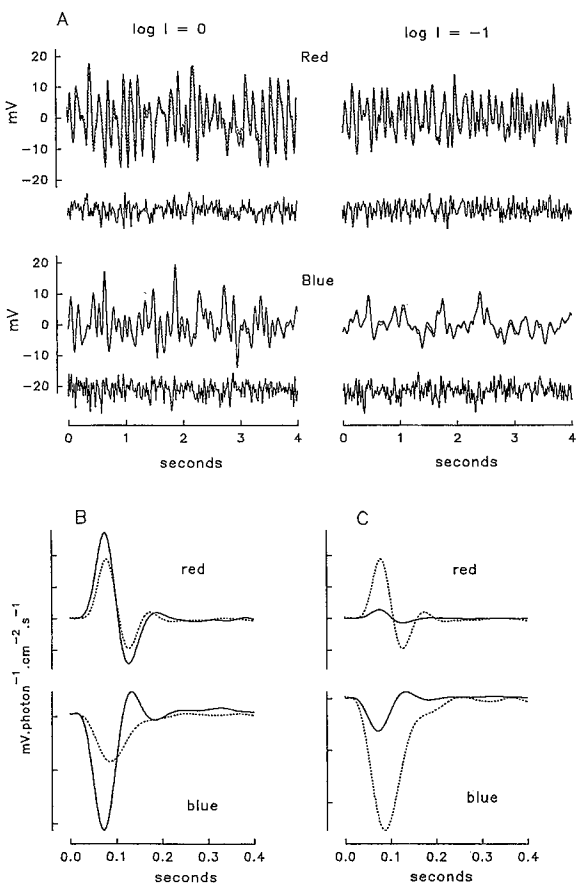

FIGURE 10. Effect of varying mean luminance of modulated input on C cell response dynamics. In this experiment, the mean luminance of one modulated input was varied by 1 log unit with neutral density filters, while the mean luminance of the opponent color remained constant. (*A*, *top*) Red white noise input at two levels of mean luminance. Red mean = 32.3 (*left*) and 3.23 (*right*) × 10^{12} photons·cm^{-2}·s^{-1}. Blue mean for both inputs = 3.23 × 10^{12} photons·cm^{-2}·s^{-1}. (*A*, *bottom*) Blue white noise input at two levels of mean luminance. Blue mean = 3.23 (*left*) and 0.32 (*right*) × 10^{12} photons·cm^{-2}·s^{-1}. Red mean for both inputs = 32.3 × 10^{12} photons·cm^{-2}·s^{-1}. For both red and blue stimuli, the input signal shown was recorded before the mean intensity of the modulated stimulus was changed with neutral density filters; therefore the amplitude of each used for the cross-correlation is the same at both intensities. Modulation depth is ~59%. Response records in *A* show first-order prediction (*dotted trace*) superimposed on real intracellular response. (*B*) Resulting first-order kernels plotted on the contrast-sensitivity scale, i.e., the input signal displayed was used for the cross-correlation without regard to attenuation. (*C*) The same first-order kernels plotted on the incremental sensitivity scale, i.e., kernel amplitude was scaled proportionately to mean intensity of modulated input. Except for Fig. 10 *B*, all kernels in this report are plotted on an incremental sensitivity scale. In *B* and *C*, the solid-line kernels are for the brighter input and the dashed-line kernels are for the dimmer input. Kernel units in *C:* red = 100; blue = 100 (these units also apply to the dashed red kernel and solid blue kernel in *B*). See text for further explanation.

prediction. For each color, the attenuated stimulus and response is shown in the right column.

Fig. 10, *B* and *C*, show the results of the cross-correlation plotted on two different scales, contrast sensitivity and incremental sensitivity, respectively. The solid-line kernel is for the brighter mean (Fig. 10 *A, left panels*), and the dotted-line kernel is for the attenuated input (Fig. 10 *A, right panels*). On the contrast sensitivity scale (Fig. 10 *B*), the cross-correlation was performed without correcting for the attenuation of the input signal. This is a valid measure because the neutral density filter attenuates (or increments) the intensity of the mean and modulation luminance to the same degree, so the contrast is unchanged. The kernels in Fig. 10 *C* were computed by cross-correlation of the same data after correcting for the difference in mean intensity by reducing the scale of the brighter kernels by a factor of 10. The same result could have been achieved by scaling the amplitude of each input signal before performing the cross-correlation so that it directly reflected the actual intensity of the mean luminance. As shown previously for L-HCs in other retinas (Naka, Chan, and Yasui, 1979; Chappell et al., 1985), the kernel amplitude increases with an increase in mean luminance when plotted on a contrast sensitivity scale, whereas kernel amplitude decreases with an increase in mean luminance when plotted on the incremental sensitivity scale. Thus, the effect of increasing the mean luminance on the dynamics of C-HCs is similar to that reported for L-HCs: (*a*) the amplitude of the modulation response increases with an increase of the mean luminance but the incremental sensitivity decreases; and (*b*) with a brighter mean luminance, the time to peak decreases and the kernel waveform becomes more biphasic. In Fig. 10 *C*, note that a 10-fold increase in mean light intensity results in only a twofold increase (or less) in the amplitude of the modulation response, yet the decrease in incremental sensitivity) is much greater. Also note that transmission is still linear at the two means, at least for the intensities tested here.

Fig. 11 shows an experiment in which each colored input was modulated in the presence and absence of a mean luminance by the opponent color. The input stimuli and resulting intracellular responses are displayed on the same amplitude and time scale. In Fig. 11 *A*, the red white noise input was modulated in the presence (left) and absence (right) of the blue mean. The blue mean hyperpolarized the membrane potential by −26 mV compared to when the mean was off. In Fig. 11 *B*, the blue white noise input was modulated in the presence (left) and absence (right) of the red mean. The red mean depolarized the cell by +18 mV compared to when the mean was off. Despite the large changes in mean membrane potential induced by adding or removing a mean luminance of the opponent color, there were relatively minor changes in the modulation responses under these different conditions (also see Fig. 3). Moreover, note that the linear prediction (*dotted line* in all response traces) still closely matches the intracellular response under all four conditions.

Fig. 11 *C* shows the first-order kernels computed under the four different stimulus conditions, and they are plotted on the same incremental sensitivity scale. For both red (left) and blue (right) sets, the solid-line kernels were computed in the presence of the opponent mean, and the dashed-line kernels were computed with the opponent mean off. In the absence of a blue mean, the amplitude of the red kernel was reduced, the time to peak increased, and the width broadened slightly (frequency

response decreased). This effect resembles the effect of reducing the mean intensity of the red stimulus in Fig. 10. For the case of the blue modulation response (Fig. 11 *C*, *right*), removing the red mean had a less pronounced effect on the blue response dynamics. The amplitude of the blue kernel was reduced only slightly, and there was a small decrease in kernel width. Similar findings were observed in two other retinas tested in the presence and absence of the opponent mean.

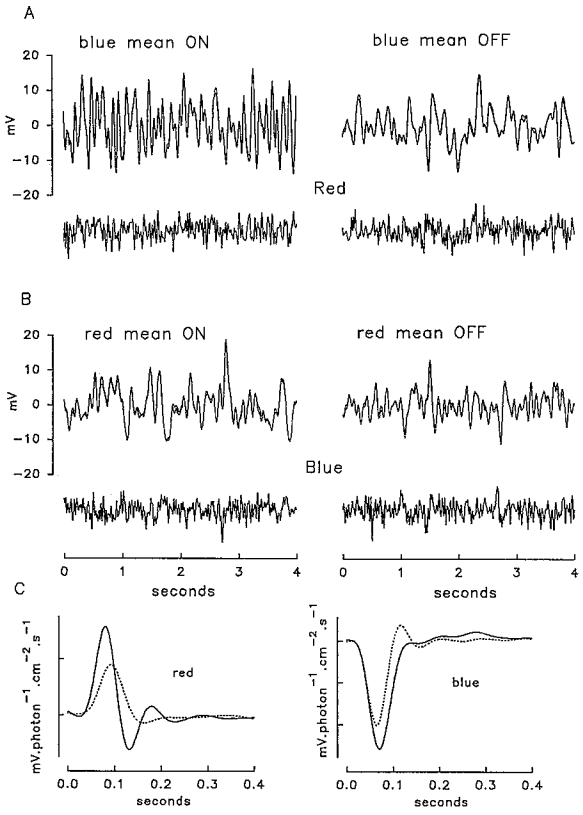

FIGURE 11. Effect of removing mean luminance of one color during white noise–modulated input by the opponent color. (*A*) Red white noise input in presence (*left*) and absence (*right*) of a blue mean luminance. (*B*) Blue white noise input in presence (*left*) and absence (*right*) of a red mean luminance. In *A* and *B*, response records show actual intracellular response (*solid line*) and first-order prediction (*dotted line*). Intracellular responses and linear predictions in *A* and *B* are plotted on the same millivolt scale. (*C*) Red (*left*) and blue (*right*) first-order kernels computed from the data in *A* and *B*, and plotted on the same incremental sensitivity scale. The solid-line kernels were computed in the presence of an opponent mean luminance (*A* and *B*, *right records*) and the dashed-line kernels were computed in the absence of an opponent mean (*A* and *B*, *right records*). Mean light intensity (*A* and *B*) (photons × 10^{12}·cm^{-2}·s^{-1}): red = 3.23, blue = 1.1. Modulation depth is ~54%. Kernel units (mV/photon × 10^{12}·cm^{-2}·s^{-1}): red = 95, blue = 105. See text for further explanation.

The reasons for these effects are not clear. They may be related to the difference in mean membrane potential under the different stimulus conditions, but it is possible that additional factors are involved, possibly differences in adaptational and phototransduction mechanisms in the red and blue photoreceptors (Tranchina et al., 1984; Perry and Mcnaughton, 1991). Also, it is interesting to note that the effect of a blue background on the red response dynamics resembles the rod-dependent enhancement of L-HC responses (Witkovsky and Stone, 1987; Frumkes and Eysteinsson, 1987; Witkovsky, Stone, and Tranchina, 1989), although at this time there is insufficient evidence to suggest that both short wavelength–dependent phenomena

are related. This observation is unlikely to result from changes in L-HC membrane potential because L-HCs are insensitive to blue light but very sensitive to red light under these conditions (see below). When the unmodulated mean luminance was increased or decreased by only 1 log unit (removing the unmodulated mean completely represents the extreme condition), there were only minimal changes in the dynamics of the modulation responses (not illustrated).

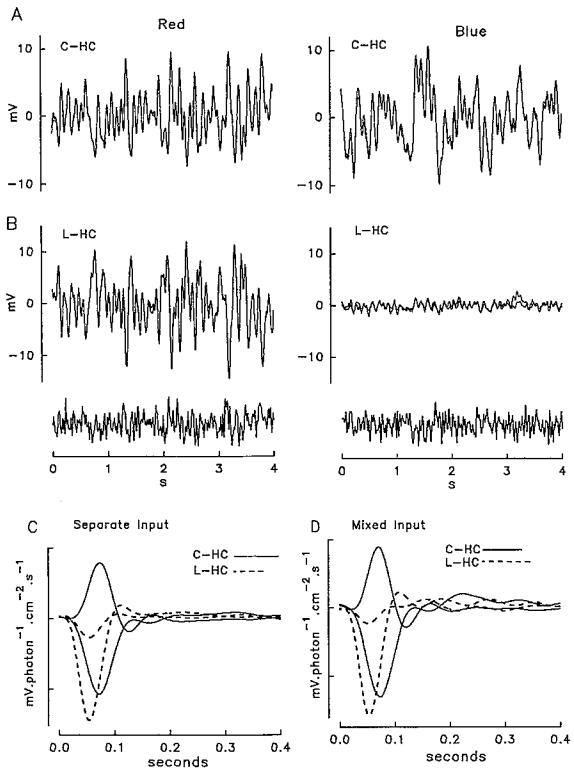

FIGURE 12. *A* and *B* show simultaneous intracellular recording from L-type horizontal cell (L-HC) and C-type horizontal cell (C-HC) during stimulation with white noise–modulated light. (*A*) Intracellular response (*solid trace*) and linear model (*dotted trace*) of C-HC in response to red (*left*) and blue (*right*) white noise inputs in the presence of a mean luminance by the opponent color. (*B*) Intracellular response (*solid trace*) and linear model (*dotted trace*) of L-HC recorded simultaneously with the C-HC in *A*. The red and blue stimulus is displayed beneath the response records in *B*. (*C*) First-order kernels computed from the separate input data shown in *A* and *B* plotted on the same incremental sensitivity scale. The solid-line kernels are for the C cell and the dashed-line kernels are for the L-HC. (*D*) First-order kernels computed from simultaneous red and blue inputs (white noise data not shown). Mean light intensity for *A* and *B* (photons × 10^{12}·cm^{-2}·s^{-1}): red = 3.23, blue = 1.1. Modulation depth approximately 54%. Kernel units (mV/photon × 10^{12}·cm^{-2}·s^{-1}) = 200.

Comparison with Luminosity-type Horizontal Cells

In other species, it is widely believed that the blue (hyperpolarizing) signal in biphasic C-HCs is produced by direct synaptic input from a short wavelength–sensitive cone, whereas the red cone signal (depolarizing) is transmitted via L-HCs (Baylor, Fuortes, and O'Bryan, 1971; Fuortes and Simon, 1974). This issue was investigated by simultaneous intracellular recordings from C-type and L-type HCs in four different retinas. An example of such an experiment is illustrated in Fig. 12, which shows simultaneous recordings from a C-HC (Fig. 12 *A*) and L-HC (Fig. 12 *B*) during stimulation with red (left) and blue (right) white noise–modulated light in the presence of mean illumination by the opponent color. The left records in *A* and *B*

show that the same red white noise input (*bottom trace*) results in large modulation responses from both C-type and L-type HCs. For both cell types, the linear prediction (*dotted trace* in each response record) closely matches the real intracellular response. In contrast, the modulation responses evoked by the blue white noise input (*A* and *B, right records*) are very different in the two cell types. The C-HC responds vigorously to the blue input (response range >20 mV), whereas the modulation response from the L-HC is <2 mV. In the L-HC (Fig. 12 *B*), the linear prediction for the blue response (MSE = 60%) does not match as well as the red (MSE = 3.5%) because of the poor signal noise ratio for the smaller blue modulation responses.

Fig. 12 *C* shows the first-order kernels computed from the data in *A* and *B* that were used to compute the linear model. The four kernels are plotted on the same incremental sensitivity scale; the solid-line kernels are for the C-HC, and the dashed-line kernels are for the L-HC. Fig. 12 *D* shows the kernels produced when the same red and blue inputs were presented simultaneously (raw data not shown), as described for the dual input experiment in Fig. 6. The similarity of the kernels in *C* and *D* demonstrates that the analysis is capable of dissecting out the separate response components, even for the very small blue component in the L-HC response.

There are several additional points worth noting in Fig. 12, *C* and *D:* (*a*) In the L-HC, the incremental sensitivity for red light is much greater than for blue; however, the dynamics of the red and blue responses are identical. If the red and blue L-HC kernels are plotted on a normalized scale, their waveforms are identical (not illustrated). This is consistent with the concept of univariance for the L-HC signal, i.e., under these light-adapted conditions, the red and blue response components are generated by the same red-sensitive cone.

(*b*) For the L-HC kernel, the time to peak was always shorter than either the red or blue C-HC kernel. Also, the frequency response of the L-HC signal was faster than the blue C-HC signal. This is consistent with the hypothesis that hyperpolarizing inputs in the L-HC and C-HC are mediated by direct synaptic input from a red- and blue-sensitive cone, respectively (Stone et al., 1990), and these two classes of cones may have different response dynamics (Perry and McNaughton, 1991).

(*c*) Although the red C-HC kernel and the red L-HC kernel were of opposite polarity and differed in their amplitude, i.e., incremental sensitivity, they both showed similar bandpass properties. Also, in all four C-HC/L-HC pairs studied, the frequency response of the red C-HC modulation response often closely approached that of the red L-HC modulation response, but never exceeded it. These similarities in red response dynamics suggest that the hyperpolarizing L-HC signal may contribute to the generation of the red (depolarizing) C-HC response.

DISCUSSION

Linearity of C Cell Modulation Responses

The results of this study demonstrate the linear transmission of red and blue signals to C-HCs (and L-HCs) for modulation responses up to ±20 mV. Furthermore, such linear behavior was observed over a wide range in mean membrane potentials (e.g., Figs. 3, 10, and 11) that encompass virtually the entire operating range of the horizontal cell. Thus, except for the polarity of the red C-HC signal (i.e., depolariz-

ing), the dynamic features of C-HC response are similar to L-HCs when the input stimulus is a modulation around a mean luminance. In turtle L-HCs, Tranchina et al. (1981, 1983) reached the same conclusion using a sinusoidally modulated input, and there have been many studies in several retinas demonstrating that photoreceptors, L-HCs and bipolar cells respond linearly when a white noise–modulated input is used as the light stimulus (reviewed in Sakai and Naka, 1988). In the *Xenopus* retina (unpublished data), the response dynamics of light-adapted L-HCs are very similar to the findings of Chappell et al. (1985) and Tranchina et al. (1981, 1983) for L-HCs in turtle retina. A perplexing issue is why are the modulation responses of horizontal cells so linear when there is a large body of evidence that voltage-dependent conductances in these neurons (Winslow and Ma, 1990; Lasater, 1986; Low, Yamada, Djamgoz, 1991; Lasater and Lam, 1992; Akopian and Witkovsky, 1992) might generate nonlinear behavior in the presence of the large fluctuations in voltage shown here. Indeed, in the *Xenopus* eyecup preparation, we have shown that spike-like calcium transients are observed in L-HCs when steps of light are used as the input stimulus; these tetrodotoxin-insensitive spikes exceed 30 mV in the presence of strontium ions (Stone et al., 1987). Clearly, such nonlinear behavior is not observed in the same eyecup preparation when the light stimulus is a modulated input. If these voltage-dependent conductances are active, they operate within their linear range most of the time. It seems likely that the experimental conditions used in the present study more closely resemble the physiological condition in vivo. Apparently, any tendency of C-HCs (or L-HCs) to display nonlinear behavior is suppressed or masked under light-adapted conditions when the light stimulus is a modulation around a mean luminance.

Differences in Red and Blue Response Dynamics: Implications for Underlying Pathways

Two differences in the response dynamics of the red and blue C-HC signals were consistently observed: (*a*) the frequency response of the blue signal was slower than for the red; and (*b*) the red kernel was more bandpass (differentiating) than the blue kernel. In addition, there was little or no interaction between the red and blue modulation responses, and the amplitude of the red or blue modulation response did not appear to depend greatly on the mean membrane potential of the C-HC or the L-HC. Finally, in the L-HC, the time-to-peak (a reflection of response latency) of the L-HC kernel was always shorter than either the blue or red C-HC kernel.

Origin of the Blue C-HC Signal

In biphasic C-HCs from turtle and fish, the short wavelength input (hyperpolarizing input) is generated by direct synaptic input from a short wavelength (blue or green) cone (Stell and Lightfoot, 1975; Ohtsuka and Kouyama, 1986; Djamgoz and Downing, 1988). Because *Xenopus* and other amphibians (Denton and Wyllie, 1955; Witkovsky, Levine, Engbretson, Hassin and MacNichol, 1981) are known to possess blue-sensitive rods in addition to the more common green-sensitive rod and red-sensitive cone, in the past, it had been reasonable to assume that the blue signal was generated by synaptic input from the blue-sensitive rod. However, more recent spectrophotometric (Hárosi, 1982) and immunocytochemical evidence (Röhlich, Szél,

and Papermaster, 1989) indicates that amphibians, including *Xenopus* (Witkovsky, P., personal communication) also possess a blue-sensitive cone, and recent studies of isolated cones from tiger salamander (Perry and McNaughton, 1991) show that the kinetics of light-activated currents from such blue-sensitive cones are much slower than that of red-sensitive cones. This strongly suggests that the source of the blue-sensitive signal in *Xenopus* C-HCs is direct synaptic input from a blue-sensitive cone whose response dynamics are slower than that of the red-sensitive cone. The blue C-HC signal is very conelike in that it is virtually impossible to suppress with bright light ($>10^{13}$ photons·cm^{-2}·s^{-1}) (Stone et al., 1990). On the other hand, in *Xenopus,* recent electron microscopic studies of HRP-injected C-HCs reveal that this cell receives input from both rod and cone photoreceptors (Stone and Witkovsky, unpublished data). However, the spectral class of the rod and cone photoreceptor(s) providing direct input to C-HCs, as well as their role in the generation the C-HC light response, remains to be established. The EM studies by Ogden et al. (1985) have also demonstrated mixed input from rods and cones to C-HCs in *Rana pipeans.*

Origin of the Red C-HC Signal

The frequency response and bandpass characteristics of the red C-HC modulation response is similar to that of L-HCs. Thus, it seems reasonable to assume that light absorption by the same red cone is responsible for the depolarizing signal in C-HCs and the hyperpolarizing signal in L-HCs. Three possible pathways (not mutually exclusive) could be responsible for generating the red (depolarizing) C-HC signal: (*a*) A sign-inverting feedback pathway from the L-HC onto the short wavelength cone (Baylor et al., 1971; Fuortes and Simon, 1974; Stell, Lightfoot, Wheeler and Leeper, 1975). This is the most widely held view. However, because biphasic C-HCs in turtle and some fish contact multiple cone types, the exclusive role of feedback to cones in generating color opponency has been questioned (Ohtsuka and Kouyama, 1986; Kammermans et al., 1991; Burkhardt, 1993; Millar and Anderson, 1991). (*b*) A direct sign-inverting input from the L-HC onto the C-HC or nonsynaptic ephaptic interactions resulting from extracellular current flow, as suggested by Byzov and Shura-Bura (1986). There is no direct evidence to support such a pathway, but there is none to refute it either. (*c*) Direct synaptic input from a blue-sensitive cone and a red-sensitive cone. This is consistent with the difference in the response dynamics of blue and red cones shown by Perry and McNaughton (1991) in tiger salamander, and is also consistent with our earlier pharmacological study suggesting the red and blue C-HC inputs may be electrically isolated from each other (Stone et al., 1990). To produce opposite polarity responses, a direct input from two cone types would require that they use different neurotransmitters or that their postsynaptic receptors (presumably to glutamate) activate different ionic currents (Yamada, Djamgoz, Low, Furukawa, and Yasui, 1991). Thus far, the pharmacological evidence in *Xenopus* regarding distinct glutamate receptors on C-HCs is inconclusive. The red C-HC signal is insensitive to the glutamate analogue APB, so it is not similar to the glutamate receptor on depolarizing bipolar cells (Slaughter and Miller, 1981), and no agent has been found that blocks the blue (hyperpolarizing) signal, leaving the red (depolarizing) signal intact (Stone et al., 1990). On the contrary, pharmacological agents such as glycine and glutamate antagonists, which block the L-HC signal, also eliminate the

red C-HC response (Stone et al., 1990). This supports (but does not prove) a underlying role for L-HCs in producing the red C-HC response.

The finding that red (and blue) L-HC kernels were always faster than blue C-HC kernels (Fig. 12) is consistent with a role of the L-HC is generating the red C-HC signal, but these data cannot distinguish between an indirect, sign-inverting feedback pathway to the blue cone (red cone to L-HC to blue cone to C-HC) or a direct sign-inverting input from the L-HC onto the C-HC. If the red signal in the C-HC is due solely to feedback to cones, then the present findings indicate that the feedback synapse operates over a linear range for large polarizations in L-HC membrane potential (>40 mV), as does the direct synapse from cones to horizontal cells. Also, such feedback transmission must permit a response to red light that is faster than the response to blue light.

According to the feedback hypothesis, the same blue-sensitive cone must be responsible for transmitting both hyperpolarizing and depolarizing signals in the C-HC. The hyperpolarizing (blue) signal is transmitted via direct sign-conserving input from the blue cone to the C-HC, and the depolarizing (red) signal is transmitted via the sign-inverting feedback pathway to the blue cone. Thus, one would expect the red signal to be delayed with respect to the blue signal because of the two additional synapses involved. However, true "synaptic delay" cannot be determined from these experiments because the major portion of the response latency is caused by the phototransduction process in the red- and blue-sensitive photoreceptors, which Perry and McNaughton (1991) have shown may be different. If the red C-HC signal is caused by feedback, then the present results imply that some high pass filtering process must be operating to speed up transmission under red illumination. The observed differences in the red and blue response dynamics of the C cell are unlikely to be caused by a voltage-dependent conductance intrinsic to the C-HC membrane because the range of voltage fluctuations (both depolarizations and hyperpolarizations) in this cell is the same for both colors, and they are linear over nearly the entire operating range of the cell. The high pass filtering mechanism may be related to a slower phototransduction process in the blue cone (i.e., red light is not absorbed by the blue cone, so cone transmission to the C-HC via the feedback synapse is faster in the absence of blue light). In conclusion, any model proposed to account for color opponency in the distal retina must be able to explain these data as well.

Note added in proof: After this manuscript was submitted, a comprehensive review dealing with the topic of the role of synaptic feedback in generating depolarization and color opponency in cones, was published by D. A. Burkhardt (1993. Synaptic feedback, depolarization, and color opponency in cone photoreceptors. *Visual Neuroscience.* 10:981–989).

Dr. Burkhardt has suggested that "feedback may impress some detectable wavelength dependency in some cones but the dominant mechanisms for color opponency probably reside beyond the photoreceptors."

I am grateful to Drs. H. Sakai and K.-I. Naka for many helpful discussions and suggestions and Dr. D. Tranchina for critical reading of the manuscript. Also I thank Dr. Naka for use of the white noise function generator and PC-STAR, Mr. M. Nasu for translation of the STAR algorithms into C, and Mr. George Thomas and Mr. Bernard Bruno for construction of the LED drivers and photostimulator.

This work was supported by EY-06960, core grant EY-01842, and by an unrestricted grant from Research to Prevent Blindness, Inc. to the Department of Ophthalmology, New York University Medical Center.

Original version received 20 October 1993 and revised version received 19 January 1994.

REFERENCES

Akopian, A., and P. Witkovsky. 1992. Membrane currents of *Xenopus* retinal horizontal cells. *Society for Neuroscience Abstracts.* 18:839.

Baylor, D. A., M. G. F. Fuortes, and P. M. O'Bryan. 1971. Receptive fields of cones in the retina of the turtle. *Journal of Physiology.* 214:265–294.

Burkhardt, D. A. 1993. Synaptic feedback, depolarization, and color opponency in cone photoreceptors. *Visual Neuroscience.* 10:981–989.

Burkhardt, D. A., and G. Hassin. 1978. Influences of cones upon chromatic and luminosity-type horizontal cells in pikeperch retina. *Journal of Physiology.* 281:125–137.

Byzov, A. L., and T. M. Shura-Bura. 1986. Electrical feedback mechanism in the processing of signals in the outer plexiform layer of the retina. *Vision Research.* 26:33–44.

Chappell, R. L., K.-I. Naka, and M. Sakuranaga. 1985. Dynamics of turtle horizontal cell response. *Journal of General Physiology.* 86:423–453.

Collins, A. D., and B. B. Sawhney. 1993. Pseudorandom binary sequence stimulation applied to the visual evoked response: normative data and a comparative study with pattern and flash stimulation. *Documenta Ophthalmologica.* 83:163–173.

DeAngelis, G. C., I. Ohzawa, and R. D. Freeman. 1993. Spatiotemporal organization of simple-cell receptive fields in the cat's striate cortex. I. General characteristics and postnatal development. *Journal of Neurophysiology.* 69:1091–1117.

Denton, E. J., and J. H. Wyllie. 1955. Study of the photosensitive pigments in pink and green rods of the frog. *Journal of Physiology.* 127:81–89.

Djamgoz, M. B. A., and J. E. G. Downing. 1988. A horizontal cell selectively contacts blue-sensitive cones in cyprinid fish retina: intracellular staining with horseradish peroxidase. *Proceedings of the Royal Society of London. B: Biological Sciences.* 235:281–287.

Eggermont, J. J. 1993. Wiener and Volterra analyses applied to the auditory system. *Hearing Research.* 66:177–201.

Fain, G. L. 1975. Interactions of rod and cone signals in the mudpuppy retina. *Journal of Physiology.* 252:735–769.

Fréchet, M. 1910. Sur les fonctionelles continues. *Annales Scientifiques de l'Ecole Normal Superieure.* 27:193–216.

Frumkes, T. E., and T. Eysteinsson. 1987. Suppressive rod-cone interaction in distal vertebrate retina: intracellular records from *Xenopus* and *Necturus*. *Journal of Neurophysiology.* 57:1–23.

Fuortes, M. G. F., and E. J. Simon. 1974. Interactions leading to horizontal cell responses in the turtle retina. *Journal of Physiology.* 240:177–198.

Gottesman, J., and D. A. Burkhardt. 1987. Response properties of C-type horizontal cells in the retina of the bowfin. *Vision Research.* 27:179–189.

Hárosi, F. I. 1982. Recent results from single-cell microspectrophotometry: Cone pigments in frog, fish, and monkey. *Color Research Applications.* 7:135–141.

Jacobson, L. D., J. P. Gaska, H.-W. Chen, and D. A. Pollen. 1993. Structural testing of multi-input linear-nonlinear cascade models for cells in macaque striate cortex. *Vision Research.* 33:609–626.

Jones, J. P., and L. A. Palmer. 1987. The two-dimensional spatial structure of simple receptive fields in cat striate cortex. *Journal of Neurophysiology.* 58:1187–1211.

Kamermans, M., B. W. van Dijk, and H. Spekreijse. 1991. Color opponency in cone-driven horizontal cells in carp retina. Aspecific pathways between cones and horizontal cells. *Journal of General Physiology.* 97:819–843.

Kondoh, Y., T. Arima, J. Okuma, and Y. Hasegawa. 1993. Response dynamics and directional properties of nonspiking local interneurons in the cockroach cercal system. *Journal of Neuroscience.* 13:2287–2305.

Lasater, E. M. 1986. Ionic currents of cultured horizontal cells isolated from white perch retina. *Journal of Neurophysiology.* 55:499–513.

Lasater, E. M., and D. M. K. Lam. 1992. Membrane properties of distal retinal neurons. *Progress in Retinal Research.* 11:215–246.

Low, J. C., M. Yamada, and M. B. A. Djamgoz. 1991. Voltage clamp study of electrophysiologically-identified horizontal cells in carp retina. *Vision Research.* 31:437–449.

Marmarelis, P. Z., and K.-I. Naka. 1972. White-noise analysis of a neuron chain: an application of the Wiener theory. *Science.* 175:1276–1278.

Millar, T. S., and P. J. Anderton. 1991. Effects of excitatory amino acids and their antagonists on the light response of luminosity and color-opponent horizontal cells in the turtle (*Pseudymys scripta elegans*) retina. *Visual Neuroscience.* 6:135–149.

Miller, W. H., Y. Hashimoto, T. Saito, and T. Tomita. 1973. Physiological and morphological identification of L- and C-type S-potentials in the turtle retina. *Vision Research.* 13:433–477.

Naka, K.-I., R. Y. Chan, and S. Yasui. 1979. Adaptation in catfish retina. *Journal of Neurophysiology.* 42:441–454.

Naka, K.-I., M. A. Itoh, and R. L. Chappell. 1987. Dynamics of turtle cones. *Journal of General Physiology.* 89:321–337.

Naka, K.-I., and W. A. H. Rushton. 1966*a*. S-potentials from colour units in the retina of fish (*Cyprinidae*). *Journal of Physiology.* 185:536–555.

Naka, K.-I., and W. A. H. Rushton. 1966*b*. An attempt to analyse colour reception by electrophysiology. *Journal of Physiology.* 185:556–586.

Naka, K.-I., and H. M. Sakai. 1991. The messages in optic nerve fibers and their interpretation. *Brain Research Reviews.* 16:135–149.

Ogden, T. E., G. G. Mascetti, and R. Pierantoni. 1985. The outer horizontal cell of the frog retina: morphology, receptor input, and function. *Investigative Ophthalmology & Visual Science.* 26:643–656.

Ohtsuka, T., and N. Kouyama. 1986. Electron microscopic study of synaptic contacts between photoreceptors and HRP-filled horizontal cells in the turtle retina. *Journal of Comparative Neurology.* 250:141–156.

Perry, R. J., and P. A. McNaughton. 1991. Response properties of cones from the retina of the tiger salamander. *Journal of Physiology.* 433:561–587.

Reid, R. C., and R. M. Shapley. 1992. Spatial structure of cone inputs to receptive fields in primate lateral geniculate nucleus. *Nature.* 356:716–718.

Röhlich, P., A. Szél, and D. S. Papermaster. 1989. Immunocytochemical reactivity of *Xenopus laevis* retinal rods and cones with several monoclonal antibodies to visual pigments. *Journal of Comparative Neurology.* 290:105–117.

Sakai, H. M. 1992. White-noise analysis in neurophysiology. *Physiological Reviews.* 72:491–505.

Sakai, H. M., K.-I. Naka, and M. J. Korenberg. 1992. Dissection of a neuron network through white-noise analysis. *News in Physiological Sciences.* 7:259–264.

Sakai, H. M., and K.-I. Naka. 1987. Signal transmission in the catfish retina. V. Sensitivity and circuit. *Journal of Neurophysiology.* 58:1329–1350.

Sakai, H. M., and K.-I. Naka. 1988. Neuron network in catfish retina: 1968–1987. *Progress in Retinal Research.* 7:149–208.

Sakuranaga, M., and K.-I. Naka. 1985. Signal transmission in the catfish retina I. Transmission in the outer retina. *Journal of Neurophysiology.* 53:373–389.

Slaughter, M. M., and R. F. Miller. 1981. 2-amino-4-phosphonobutyric acid: a new pharmacological tool for retinal research. *Science.* 211:182–185.

Spekreijse, H., and A. L. Norton. 1970. The dynamic characteristics of color-coded S-potentials. *Journal of General Physiology.* 56:1–15.

Stell, W. K., D. O. Lightfoot, T. G. Wheeler, and H. F. Leeper. 1975. Goldfish retina: functional polarization of cone horizontal cell dendrites and synapses. *Science.* 190:989–990.

Stell, W. K., and D. O. Lightfoot. 1975. Color-specific interconnection of cones and horizontal cells in the retina of the goldfish. *Journal of Comparative Neurology.* 159:473–502.

Stone, S., P. Witkovsky, and M. Schütte. 1990. A chromatic horizontal cell in the *Xenopus* retina: intracellular staining and synaptic pharmacology. *Journal of Neurophysiology.* 64:1683–1694.

Stone, S., and P. Witkovsky. 1984. The actions of gamma-aminobutyric acid, glycine and their antagonists upon horizontal cells of the *Xenopus* retina. *Journal of Physiology.* 353:249–264.

Stone, S., and P. Witkovsky. 1987. Center-surround organization of *Xenopus* horizontal cells and its modification by gamma-aminobutyric acid and strontium. *Experimental Biology.* 47:1–12.

Sutter, E. E. 1987. A practical non-stochastic approach to nonlinear time-domain analysis. *In* Advanced Methods of Physiological Systems Modelling. V. Z. Marmarelis, editor. University of Southern California, Los Angeles. pp. 305–315.

Svaetichin, G., and E. F. MacNichol. 1958. Retinal mechanisms for chromatic and achromatic vision. *Annals of the New York Academy of Sciences.* 74:385–404.

Tranchina, D., J. Gordon, R. Shapley, and J.-I. Toyoda. 1981. Linear information processing in the retina: a study of horizontal cell responses. *Proceedings of the National Academy of Sciences of the United States of America.* 78:6540–6542.

Tranchina, D., J. Gordon, and R. Shapley. 1983. Spatial and temporal properties of luminosity horizontal cells in the turtle retina. *Journal of General Physiology.* 82:573–598.

Tranchina, D., J. Gordon, and R. M. Shapley. 1984. Retinal light adaption-evidence for a feedback mechanism. *Nature.* 310:314–316.

Victor, J. D. 1992. Nonlinear systems analysis in vision: Overview of kernel methods. *In* Nonlinear Vision. R. B. Pinter and B. Nabet, editors. CRC Press, Boca Raton, FL. pp. 1–37.

Victor, J. D., and B. W. Knight. 1979. Nonlinear analysis with an arbitrary stimulus ensemble. *Quarterly Journal of Applied Mathematics.* 37:113–136.

Victor, J. D., and R. M. Shapley. 1979. The nonlinear pathway of Y ganglion cells in the cat retina. *Journal of General Physiology.* 74:671–687.

Volterra, V. 1959. Theory of functionals and of integral and integro-differential equations. Dover Publications Inc., New York.

Weckström, M., E. Kouvalainen, and M. Juusola. 1992. Measurement of cell impedance in frequency domain using discontinuous current clamp and white-noise-modulated current injection. *Pflugers Archives: European Journal of Physiology.* 421:469–472.

Wiener, N. 1958. Nonlinear problems in random theory. John Wiley & Sons, Inc., New York.

Winslow, R. L., and S. Ma. 1990. Bifurcation analysis of nonlinear retinal horizontal cell models. II. Network properties. *Journal of Neurophysiology.* 64:248–261.

Witkovsky, P., J. S. Levine, G. A. Engbretson, G. Hassin, and E. F. MacNichol, Jr., 1981. A microspectrophotometric study of normal and artificial visual pigments in the photoreceptors of *Xenopus laevis*. *Vision Research.* 21:867–873.

Witkovsky, P., S. Stone, and J. C. Besharse. 1988. Dopamine modifies the balance of rod and cone inputs to horizontal cells of the *Xenopus* retina. *Brain Research.* 449:332–336.

Witkovsky, P., S. Stone, and D. Tranchina. 1989. Photoreceptor to horizontal cell synaptic transfer in the *Xenopus* retina: modulation by dopamine ligands and a circuit model for interactions of rod and cone inputs. *Journal of Neurophysiology.* 62:864–881.

Witkovsky, P., and S. Stone. 1987. GABA and glycine modify the balance of rod and cone inputs to horizontal cells in the *Xenopus* retina. *Experimental Biology.* 47:13–22.

Yamada, M., M. B. A. Djamgoz, J. C. Low, T. Furukawa, and S. Yasui. 1991. Conductance-decreasing synaptic mechanisms mediating cone input to H1 horizontal cells in carp retina. *Neuroscience Research. 15(Suppl.):*S51–S65.